ACS chemical biology

Articles

pubs.acs.org/acschemicalbiology

Photoactivatable Prodrugs of Antimelanoma Agent Vemurafenib

Rebecca Horbert,[†,§] Boris Pinchuk,[†,§] Paul Davies,[‡] Dario Alessi,[‡] and Christian Peifer*[,†]

[†]Pharmaceutical Chemistry, Christian Albrechts University, Gutenbergstraße 76, 24118 Kiel, Germany

[‡]MRC Protein Phosphorylation and Ubiquitylation Unit, College of Life Sciences, University of Dundee, Dow Street, Dundee DD1 5EH, U.K.

Supporting Information

ABSTRACT: In this study, we report on novel photoactivatable caged prodrugs of vemurafenib. This kinase inhibitor was the first approved drug for the personalized treatment of BRAF-mutated melanoma and showed impressive results in clinical studies. However, the occurrence of severe side effects and drug resistance illustrates the urgent need for innovative therapeutic approaches. To conquer these limitations, we implemented photoremovable protecting groups into vemurafenib. In general, this caging concept provides spatial and temporal control over the activation of molecules triggered by ultraviolet light. Thus, higher inhibitor concentrations in tumor tissues might be reached with less systemic effects. Our study describes the first development of caged vemurafenib prodrugs useful as pharmacological tools. We investigated their photochemical characteristics and photoactivation. *In vitro* evaluation proved the intended loss-of-function and the light-dependent recovery of efficacy in kinase and cellular assays. The reported vemurafenib photo prodrugs represent a powerful biological tool for novel pharmacological approaches in cancer research.

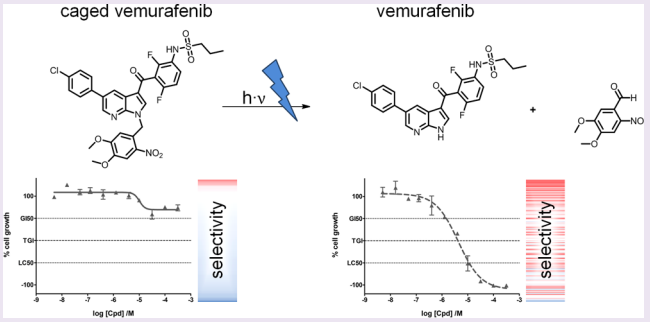

Protein kinase inhibitors have been successfully established in cancer treatment over the past 15 years. However, the occurrence of therapy-limiting side effects as well as only temporary efficacy illustrates the urgent need for novel therapeutic approaches.[1] Innovative concepts that are able to reduce adverse events and prolong duration of efficacy by overcoming tumor resistance would be of significant benefit.

Hence, we aimed to develop photoactivatable kinase inhibitor prodrugs. These so-called caged compounds can be activated by irradiation with ultraviolet (UV) light. The implementation of photoremovable protecting groups (PPGs) provides spatial and temporal control over the release of molecules. Therefore, higher drug concentrations can be reached in the area of interest, sparing other compartments.[2] This approach might enable higher drug concentrations in cancer-afflicted tissues, resulting in a faster, more efficient regression with fewer side effects. Light might be applied on superficial tumors precautionarily after surgical removal or by the use of optical fibers. Beyond novel therapeutic applications, our photo prodrugs could serve as experimental tools, e.g., for kinetic or mechanistic studies. By irradiation with a short laser impulse, the drug might be quickly released in certain tissues or organism compartments.

The photo prodrug concept is essentially based on the blockade of a pharmacophoric group. The PPG is therefore attached to the drug molecule by a covalent bond. This bond then has to be cleaved by radiant energy, releasing the parent bioactive compound. *o*-Nitrobenzylic derivatives have been widely used as PPGs in various biological applications. The first and most prominent example is certainly the photorelease of caged adenosine triphosphate (ATP) by Kaplan and co-workers in 1978.[3] Since then, intensive research has been carried out concerning various classes of protecting groups and evaluation of their photocharacteristics.[2]

While the caging concept has been successfully applied on various bioagents,[4−6] there are only a few reports on photoprotected kinase inhibitors. For instance, Morckel et al. used a photoactivatable small-molecule Rho kinase inhibitor.[7] This tool compound was used to uncover molecular mechanisms of embryonic development in *Xenopus laevis* by targeting specific regions of the living embryo.[7] In addition, small molecular equivalents of Src kinase have been caged[8] as well as peptidic PKA inhibitors.[9] Furthermore, light-regulated protein kinase C peptide-based sensors[10] and tyrosine kinase reporters[11] have been described.

In our study, we focused on $BRAF^{V600E}$ inhibitor vemurafenib (**1**, Zelboraf, Plexxikon/Roche). This serine/threonine kinase inhibitor shows excellent UV stability at 365 nm and is readily chemically accessible regarding the caging concept. Vemurafenib was the first personalized drug for the therapy of BRAF mutant cancer. It received approval for the treatment of metastatic melanoma with $BRAF^{V600}$ mutation in the United States and Europe in 2011 and 2012, respectively.[12] Introduction of vemurafenib into melanoma therapy showed

Received: March 12, 2015
Accepted: June 10, 2015
Published: June 10, 2015

DOI: 10.1021/acschembio.5b00174
ACS Chem. Biol. 2015, 10, 2099−2107

impressive clinical results.[13−15] However, despite outstanding tumor regressions and distinctive improvements in survival, vemurafenib cannot cure metastatic melanoma. Moreover, the massive dosage of up to 960 mg daily leads to a high incidence of severe adverse events such as arthralgia (joint pain), skin rash, and the development of squamous cell carcinoma.[14,16,17] Furthermore, most patients suffer from lethal relapse due to drug resistance developed after only a few months of therapy.[18−22]

Here, we report on the design, synthesis, and biological evaluation of photoactivatable prodrugs of vemurafenib. First, molecular modeling revealed promising pharmacophoric groups to be protected by PPGs. After showing the UV stability of vemurafenib at 365 nm, caged prodrugs were synthesized. In the next step, these prodrugs were photochemically characterized. This included assignment of an optimal wavelength for deprotection and investigation of photoinduced release of vemurafenib. Subsequently, determination of $BRAF^{V600E}$ K_d values and a broad kinase selectivity profile for these compounds proved the intended loss-of-function by photoprotection. Finally, recovery of vemurafenib efficacy by UV irradiation in cells could be demonstrated within proliferation assays as well as by western blot analysis.

With the presented vemurafenib photo prodrugs in hand, we have created a powerful biological tool for novel pharmacological approaches in cancer research.

RESULTS AND DISCUSSION

Molecular Modeling. We first examined ligand−protein interactions of vemurafenib in the active site of $BRAF^{V600E}$ by molecular modeling. In order to design effectless vemurafenib prodrugs, it was necessary to define key pharmacophoric moieties of this kinase inhibitor to be subsequently blocked by PPGs.

In Figure 1A,B, the binding mode of vemurafenib in the ATP pocket of $BRAF^{V600E}$ is shown (PDB code 3OG7;[23] for 2D ligand interaction diagram, see Supporting Information Figure S1). Herein, the type-I ATP-competitive inhibitor vemurafenib[23] is addressing key H-bonds by its 7-azaindole moiety toward the hinge region.[24] Furthermore, the sulfonamide NH residue of vemurafenib interacts with backbone amides of another highly conserved amino acid sequence, namely, Asp-Phe-Gly (DFG motif). This DFG motif is located at the beginning of the activation loop (A-loop), which controls substrate access to the active site.[25] Hence, both the 7-azaindole and sulfonamide are considered to be suitable pharmacophoric moieties for photoprotection. In line with this notion, modeling PPG-vemurafenib compounds **2** and **4** in the active site of $BRAF^{V600E}$ resulted in significant sterical clashes, indicating nonplausible binding modes (Figure 1C,D). However, we assumed that blocking the central azaindole-NH moiety of vemurafenib's hinge binder would demolish any affinity of the photoprotected prodrugs to every other kinase as well since all type I and II inhibitors use this interaction.[24] On the other hand, prodrugs with a PPG attached to the sulfonamide residue might still show some affinity to kinases featuring a flexible binding pocket in this peripheral area. In general, based on slight molecular differences in the kinase architecture involving shape and size of hydrophobic pockets, many tailor-made examples of highly active and selective kinase inhibitors have been developed.[1,26]

Motivated by the modeling data, we synthesized both NH-photoprotected vemurafenib analogues and compared their anticipated *in vitro* nonefficacy against the target enzyme $BRAF^{V600E}$ and within a broad kinase panel to assess their specificity.

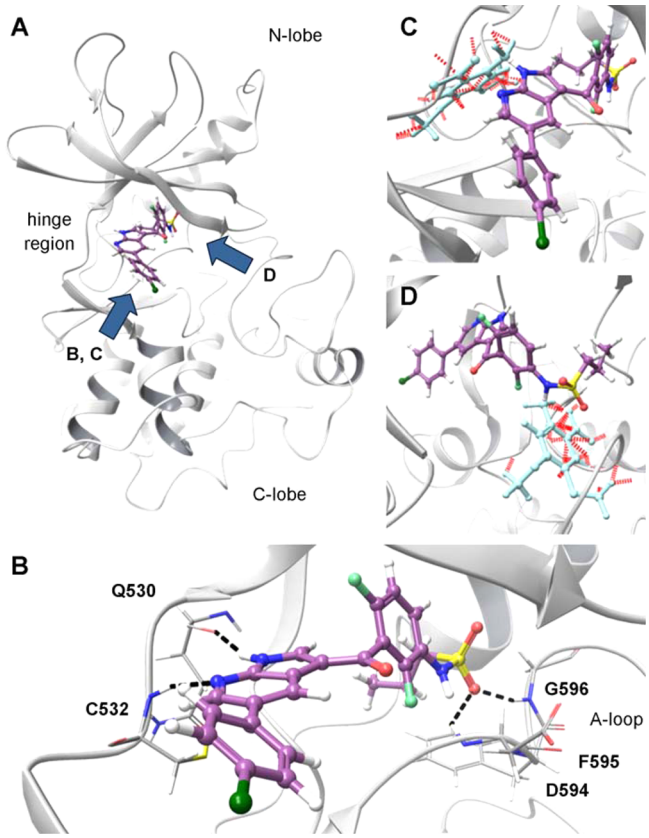

Figure 1. Binding mode of vemurafenib and determination of photoprotection sites. (A) The X-ray defined crystal structure of vemurafenib bound to the active site of $BRAF^{V600E}$ (PDB code 3OG7) is shown. Arrows indicate the perspective of the enlarged views in (B), (C), and (D). N- and C-lobe of the kinase are connected via the flexible hinge region. The ATP pocket is located in the cleft between these two subdomains, occupied by vemurafenib. (B) Detailed view of the interactions between vemurafenib and the ATP pocket. Hydrogen bonds between the ligand and the protein backbone are indicated by black dotted lines. The azaindole moiety addresses the hinge region by two key H-bonds. Access to the active site is controlled by the activation loop (A-loop), starting with the conserved amino acid sequence Asp-Phe-Gly (DFG motif). The sulfonamide residue of the ligand binds to this motif via two H-bonds. Superposition of vemurafenib with azaindole caged prodrug **2** and sulfonamide caged prodrug **4** is illustrated in (C) and (D), respectively. Red dashed lines represent sterical clashes between the PPG (photoremovable protecting group) and the target protein.

UV Stability of Vemurafenib. In general, reactivation of photoprotected prodrugs requires the parent compound's stability at the used wavelength of irradiated light. Otherwise, the drug molecule would be degraded immediately after its release or even before the bond to the PPG is cleaved. We next examined the UV stability of vemurafenib at 365 nm. For this purpose, we used a light-emitting diode (LED) reactor with a wavelength of 365 nm (5.4 W; for technical information, see Supporting Information Figures S4 and S5) to irradiate a 10 μM solution of the compound in PBS buffer containing 10% DMSO. HPLC and LC-MS analysis were used for content determination. Under these conditions, vemurafenib showed excellent stability over a period of 20 min (see Supporting

DOI: 10.1021/acschembio.5b00174
ACS Chem. Biol. 2015, 10, 2099−2107

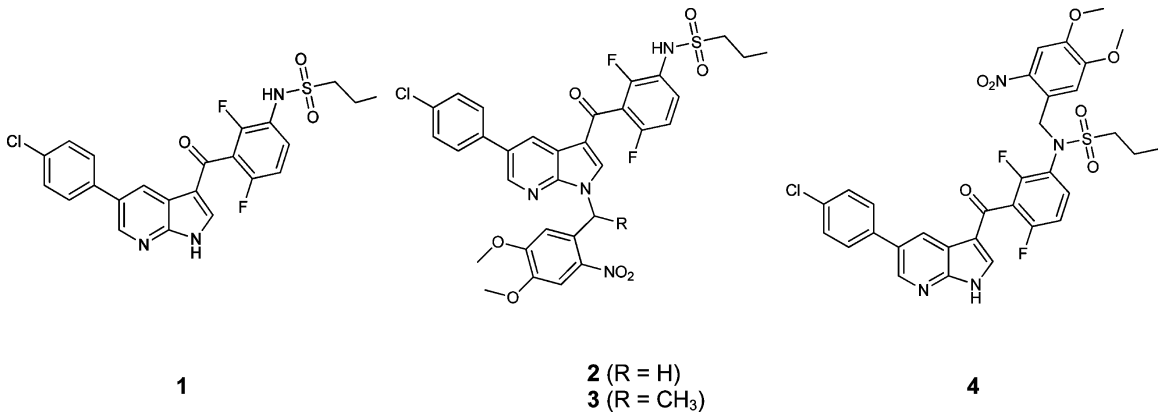

Figure 2. Chemical structures of vemurafenib (**1**), azaindole caged derivatives **2** and **3**, and sulfonamide caged **4** are shown.

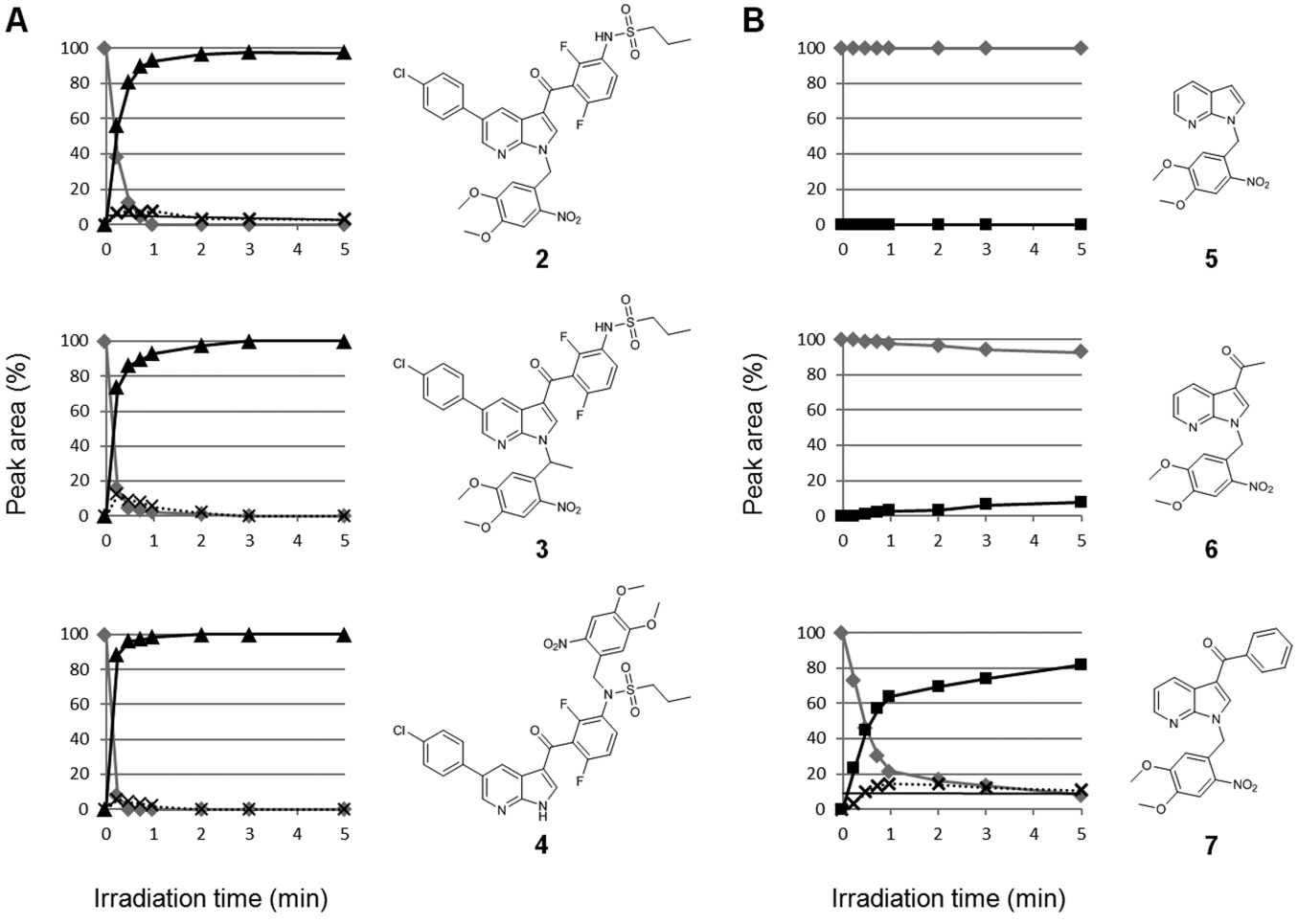

Figure 3. Photoactivation of vemurafenib prodrugs and azaindole derivatives. Uncaging was examined for photoprotected vemurafenib derivatives (A) and azaindole analogues (B). Ten micromolar compound solutions in PBS buffer containing 10% DMSO were irradiated at 365 nm (5.4 W) for 5 min and analyzed by HPLC and LC-MS. The amount of caged probe (diamonds) is plotted against released vemurafenib (triangles, A) or the corresponding azaindole analogue (squares, B), respectively. The formation of a cyclic benzisoxazolidine intermediate could be observed (crosses) and is discussed in Supporting Information Figure S10a. Photoactivation of the compounds in 1 mM DMSO solution is shown in Supporting Information Figure S10b.

Information Figures S2 and S3; for UV/vis absorption spectra of all compounds, see Supporting Information Figure S9).

Synthesis of Caged Prodrugs. Investigation of the binding mode revealed that both NH moieties within the vemurafenib structure should be suitable for the caging concept. Therefore, these functions were protected by PPGs via nucleophilic substitution. We introduced two related *o*-nitrobenzylic PPGs into the vemurafenib molecule, namely, the 4,5-dimethoxy-2-nitrobenzyl (DMNB) and 4,5-dimethoxy-2-nitrophenylethyl (DMNPE) moieties (Figure 2).

Both azaindole (**2**) and sulfonamide (**4**) DMNB photoprotected vemurafenib prodrugs could be synthesized (for

DOI: 10.1021/acschembio.5b00174
ACS Chem. Biol. 2015, 10, 2099−2107

details, see Supporting Information Figure S6 and Supporting Information section 4). These two compounds enabled a comparison to be made between the different protection sites concerning their photorelease characteristics and their biological evaluation, respectively. Through irradiation, the DMNB group produces a nitroso-benzaldehyde, whereas a less toxic ketone is released by the DMNPE moiety.[2] Therefore, the DMNPE azaindole caged vemurafenib (**3**) was synthesized as well. It is noteworthy that due to sterical hindrance at the sulfonamide only the azaindole DMNPE protected derivative was obtained (as discussed in Supporting Information Figures S7 and S8).

These photo prodrugs were subjected to further photochemical and biological evaluation.

Photochemical Characterization of Caged Prodrugs. In the following step, we investigated the photorelease kinetics of **2**, **3**, and **4**. For the prodrug concept, it is essential for the parent compound to be released rapidly and quantitatively upon irradiation. Wavelengths shorter than 300 nm might damage tissues or proteins. For the photorelease experiments, we used an LED reactor with an emission at 365 nm to irradiate 10 μM solutions of the compounds in PBS buffer containing 10% DMSO (for technical information, see Supporting Information Figure S4 and S5; for the experiment in pure DMSO, see Supporting Information Figure S10b). This wavelength has been described for the cleavage of the inserted PPGs, both DMNB and DMNPE.[2]

The results of photoinduced release of vemurafenib by our photo prodrugs are presented in Figure 3A. Upon irradiation, sulfonamide protected derivative **4** showed the fastest cleavage of the PPG. After 30 s, more than 90% of vemurafenib was released. Azaindole protected **2** and **3** were comparable to each other in their photocharacteristics. More than 90% of vemurafenib was released within 1 min. In the literature, DMNPE is reported to have a higher quantum yield compared to that of DMNB.[2] However, the assumption that **3** would show faster releasing characteristics than **2** could not be confirmed in our study. According to LC-MS and NMR studies, the formation of a cyclic benzisoxazolidine intermediate could be observed (for details, see Supporting Information Figure S10a).

In order to investigate the minimal structural requirement for the photoreaction, we investigated the vemurafenib scaffold in more detail. In general, N-heterocycles are rarely described leaving groups in photochemistry. We therefore synthesized several azaindole analogues and characterized their photochemical behavior. As illustrated in Figure 3B, caged 7-azaindole **5** was perfectly stable against UV irradiation and did not show any conversion. Photoprotected 3-acetyl-7-azaindole **6** could be uncaged but at a slow reaction rate. However, 3-benzoyl-7-azaindole **7** offered slightly slower photorelease characteristics compared to those of the vemurafenib prodrugs. This motif, therefore, can be considered to be the essential fragment for suitable photorelease of the N-heterocycle in this system.

In conclusion, both NH photoprotection sites within the investigated prodrugs proved to be suitable for rapid and quantitative photorelease. The next question addressed was whether the protection of the NH moieties in vemurafenib would actually diminish the effect on $BRAF^{V600E}$ and also suppress the antiproliferative effect in cells.

Kinase Assays. We therefore determined the binding affinity of caged and uncaged compounds toward $BRAF^{V600E}$ in a commercially available assay (for details, see Supporting Information). The $BRAF^{V600E}$ K_d values were measured as follows: 10 nM for vemurafenib, 440 nM for **2**, 77 nM for **3**, and 79 nM for **4**, respectively. In line with the modeling data, the caged compounds exhibited a lower binding affinity toward $BRAF^{V600E}$ in comparison to that for vemurafenib. The lowest binding affinity was found for azaindole protected compound **2**. This is strong evidence that protection of the azaindole moiety forestalls the inhibitor−enzyme interaction. Surprisingly, compounds **3** and **4** still show unexpected binding toward $BRAF^{V600E}$, although their affinities are significantly less than that of vemurafenib. The determined affinities can be explained by minute quantities of unprotected active compound in the samples and/or instability of caged compounds resulting in the release of vemurafenib under the assay conditions.

Subsequently, a selectivity profile over 140 kinases for vemurafenib, **2**, and **4** was performed. The results are presented in a heat map in Figure 4 (for the complete data set, see Supporting Information Table S1). Apparently, vemurafenib at

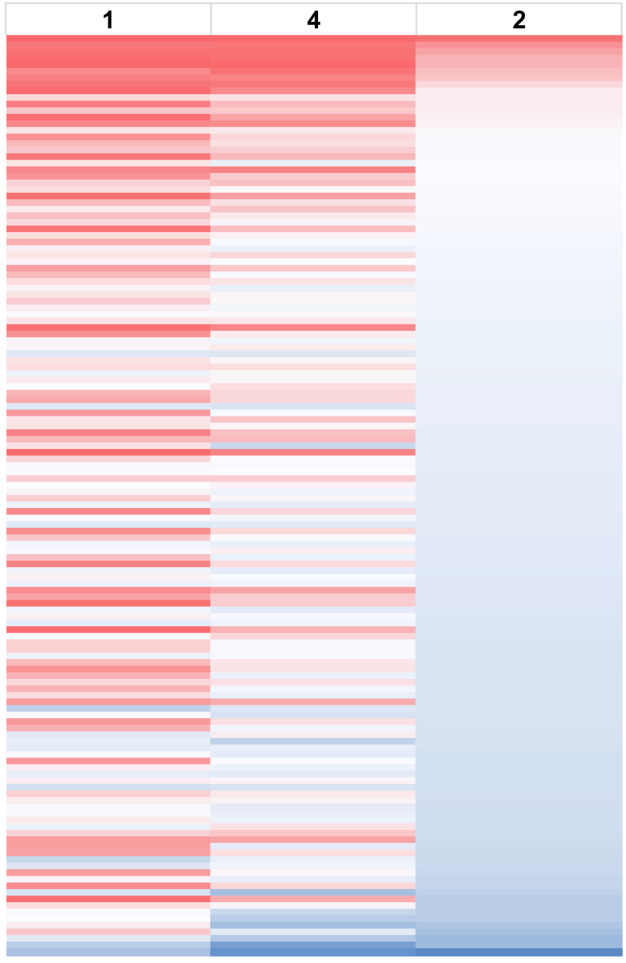

Figure 4. Kinase selectivity profiling of vemurafenib and caged prodrugs. The inhibitory effect of active vemurafenib (**1**) and caged derivatives **2** and **4** was tested in a panel of 140 kinases. The residual activity of kinases was measured after incubation with 10 μM of each compound. The data is portrayed as a heat map of the mean activity of assay duplicates. The color code refers to the residual kinase activity ranging from red (low residual activity) to blue (high residual activity). Apparently, **2** inhibits significantly less kinases than does vemurafenib and **4**.

DOI: 10.1021/acschembio.5b00174
ACS Chem. Biol. 2015, 10, 2099−2107

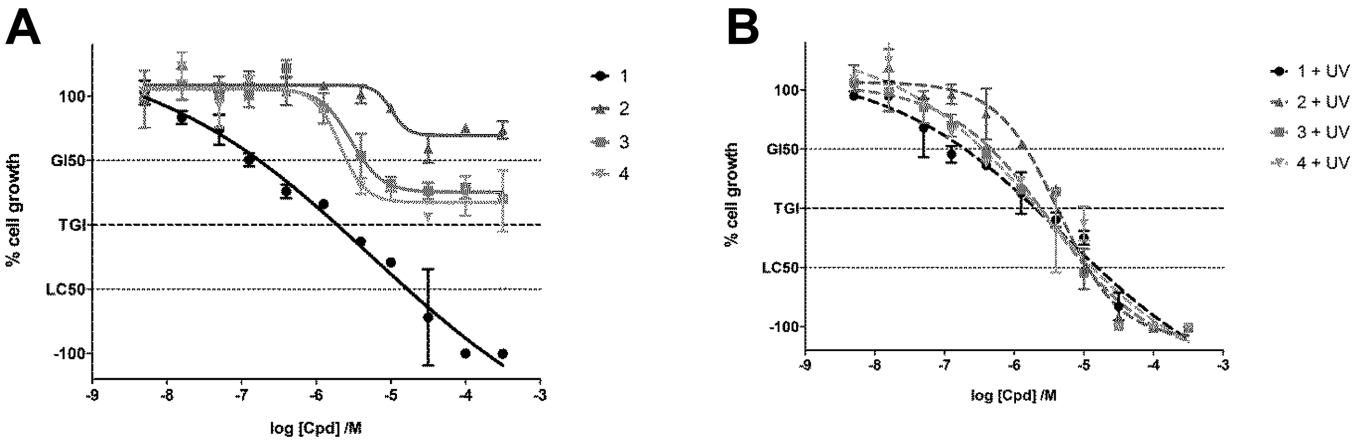

Figure 5. Activation of caged prodrugs in cell proliferation assays. The recovery of vemurafenib's efficacy by UV irradiation was demonstrated using SKMel13 cells. (A) Dose−response curves of vemurafenib (**1**) and caged prodrugs **2**, **3**, and **4** were determined without UV irradiation. Cell growth was measured 48 h after incubation with the compounds. Vemurafenib clearly shows cytotoxic effects at concentrations above 1 μM. The caged derivatives do not exhibit cytotoxic activity: the TGI mark is not reached even at high concentrations. (B) Cells were incubated for 1 h with the compounds and then irradiated at 365 nm (1.8 W) for 5 min. Cell growth was determined 48 h after incubation with the compounds. After irradiation, the caged derivatives show similar dose−response curves as that of active vemurafenib. GI_{50} = 50% growth inhibition; TGI = total growth inhibition; LC_{50} = 50% lethal concentration; n = 4. Error bars represent standard deviation.

10 μM potently inhibits several other kinases besides $BRAF^{V600E}$. Altogether, there are 32 kinases whose activities are reduced to less than 30% under the test conditions. The most affected kinases are BRK, MAP4K5, and DDR2. This data clearly indicates that vemurafenib is not highly selective at the tested concentrations in biochemical assays.

Sulfonamide caged compound **4** reduces the activity of 13 kinases to less than 30%. Its inhibitory potency against nontarget kinases is diminished in comparison to that of vemurafenib. However, some nonspecific interactions are still observable. Regarding this data, it can be assumed that protection of the sulfonamide residue prevents binding to $BRAF^{V600E}$ but is still not sufficient enough to completely suppress inhibition of other kinases.

In contrast, azaindole protected compound **2** inhibits only two kinases: MAP4K5 (7% residual activity) and RIPK2 (26% residual activity). These findings are in line with the initial assumption that blockade of the hinge binder, the azaindole moiety, would annihilate the affinity to kinases in general more effectively than the protection of the sulfonamide residue.

Cellular Assays. On the basis of the biochemical data, we supposed that the caged derivatives **2**, **3**, and **4** should show considerably less activity in cellular assays compared to that of vemurafenib. To prove this hypothesis, we investigated the antiproliferative activity of the four compounds in cellular growth assays using the melanoma cell line SKMel13, which carries the $BRAF^{V600E}$ mutation.[27] Dose−response curves for the nonirradiated compounds were measured (Figure 5A).

Vemurafenib shows potent cytotoxic activity (GI_{50} value 0.17 μM). This finding corresponds with previous studies, that revealed a strong inhibition of V600E-positive melanoma cells by vemurafenib.[28−30] In contrast, caged **2**, **3**, and **4** exhibit no cell toxicity toward the melanoma cells in the nanomolar range (Figure 5A). Cytostatic effects occur at considerably higher concentrations (GI_{50} values: 4.3 μM for **3** and 2.6 μM for **4**). Compound **2** does not show cell growth inhibition at all. Similar results could be reproduced with other V600E-positive melanoma cell lines: SKMel28, M14, and UACC62 (data shown in Supporting Information Table S2). Again, the marginal cytostatic effects of the caged probes at higher concentrations could be caused by minute impurities of unprotected vemurafenib or by off-target effects of the compounds.

Next, we examined whether the inhibitory potency of the photoprotected compounds in cells could be restored upon UV irradiation. The cell growth assays described above were performed by irradiating the cells with UV light at 365 nm (1.8 W, 5 min) with and without compound incubation. The dose−response curves are presented in Figure 5B. In this assay, the UV irradiation at the applied dosage is well-tolerated by the cells. After UV irradiation, **2**, **3**, and **4** show antiproliferative activity comparable to that of unprotected vemurafenib (GI_{50} values: 0.19 μM for vemurafenib, 1.5 μM for **2**, 0.46 μM for **3**, and 0.35 μM for **4**; Figure 5B). The slightly reduced activity in comparison to that of vemurafenib might be explained by incomplete photorelease under the described conditions.

Summarizing the results of the proliferative cell assays, it can be postulated that the irradiation of the caged compounds restores the potent activity of vemurafenib.

Having demonstrated the photoactivation of vemurafenib from its caged prodrugs, we investigated the effect of the cleaved PPG moieties on cellular growth. Caged **2**, **3**, and **4** were not suitable to answer this question because of the intrinsic toxicity of the uncaged vemurafenib after irradiation. We therefore used two model compounds: Boc protected L-alanine (Boc-Ala) and its DMNB photoprotected derivative (Boc-Ala-DMNB), as we considered Boc-Ala to be nontoxic (Supporting Information Figure S11). At first, the effect of UV-light-unexposed compounds on proliferation of the SKMel13 cells was measured. Both protected amino acid derivatives did not show any antiproliferative effects even at high concentrations. The same experiment was repeated implementing UV irradiation (365 nm, 1.8 W). Irradiated Boc-Ala is still neither cytotoxic nor cytostatic. In contrast, Boc-Ala-DMNB exhibits distinct antiproliferative activity after irradiation at concentrations above 10 μM (GI_{50} = 34.4 μM). Therefore, it can be assumed that the measured cell toxicity is caused by the cleaved DMNB. However, the concentration at which the PPG shows toxicity (10 μM) is approximately 100-fold higher than the

DOI: 10.1021/acschembio.5b00174
ACS Chem. Biol. 2015, 10, 2099−2107

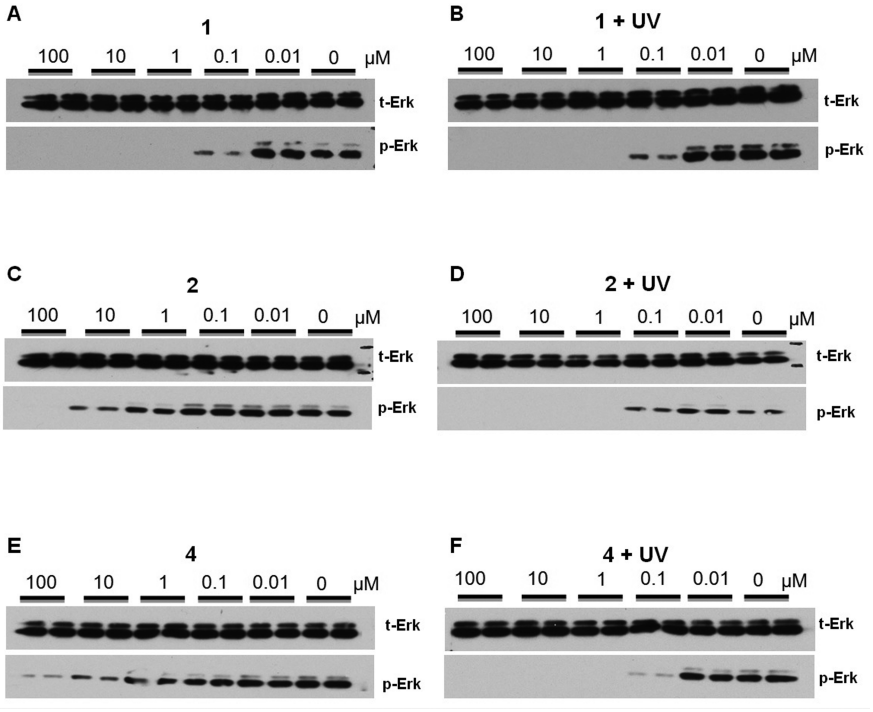

Figure 6. Activation of inhibitory effect of caged prodrugs on $BRAF^{V600E}$ signaling *in vitro*. SKMel13 cells were treated for 1 h at 37 °C with the indicated concentrations of vemurafenib (**1**) and caged prodrugs **2** and **4**. Subsequently, cells were lysed and immunoblotted. (A, C, E) Cells were incubated with the corresponding compound without irradiation. (B, D, F) Cells were incubated with the corresponding compound for 1 h, irradiated at 365 nm (1.8 W) for 5 min, and after a further 1 h of incubation, lysed and immunoblotted. The experiments were carried out in duplicates. t-Erk = total Erk; p-Erk = phosphorylated Erk. For compound **3**, see Supporting Information Figure S12. For phosphorylation of Akt, see Supporting Information Figures S13 and S14.

efficacious concentration of the released vemurafenib (0.17 μM).

Western Blots. In order to investigate the impact of vemurafenib and its caged derivatives on $BRAF^{V600E}$ signaling, we performed western blot analysis, including the phosphorylation of ERK as a readout downstream of BRAF. The results for vemurafenib, **2**, and **4** are shown in Figure 6 (for **3**, see Supporting Information Figure S12).

Initially, ERK phosphorylation in SKMel13 cells was investigated after incubation with nonirradiated compounds. Total ERK was used as a loading control. As reported for a BRAF inhibitor,[23,28−30] vemurafenib displays dose-dependent pERK inhibition at concentrations higher than 0.01 μM. The phosphorylation of ERK is completely blocked at concentrations above 0.1 μM.

According to the biochemical data, the caged compounds reveal significantly less inhibition of ERK phosphorylation. Even at a concentration of 10 μM, there are detectable signals of pERK. Consecutively, ERK phosphorylation in cells was surveyed after incubation with compounds and subsequent UV irradiation. No alteration in pERK inhibition by vemurafenib could be determined with or without irradiation. This demonstrates that the amount of phosphorylated ERK is not dependent on UV irradiation under the described conditions.

After UV irradiation, **2**, **3**, and **4** exhibit the same inhibitory potency on pERK as that of active vemurafenib. The complete suppression of ERK phosphorylation could be demonstrated at concentrations above 0.1 μM. Dose dependency correlates with that of vemurafenib.

This indicates that the inhibitory efficacy of vemurafenib on $BRAF^{V600E}$ signaling can be completely reactivated upon irradiation of the caged derivatives with UV light.

Both vemurafenib and its caged compounds exhibit no effect on the phosphorylation of Akt independent from UV irradiation (see Supporting Information Figures S13 and S14).

Conclusions. In this article, we describe the design, synthesis, and photochemical and *in vitro* characterization of novel caged prodrugs of the kinase inhibitor vemurafenib. Molecular modeling studies predicted the obviation of inhibitory potency after insertion of a PPG into vemurafenib. After UV stability of vemurafenib and photoactivation of the caged inhibitors had been confirmed, the compounds were tested in different *in vitro* assays.

In kinase binding assays, selectivity profiling, cellular assays, and western blot analysis, we demonstrated that the insertion of a PPG significantly diminishes the inhibitory efficacy and promiscuity of vemurafenib. In particular, azaindole protected compound **2** revealed hardly measurable activities even at high concentrations, both in biochemical and cellular assays. The nonspecific interactions toward off-target kinases could be drastically reduced by protecting the hinge binder, the azaindole moiety. Finally, we could clearly demonstrate that UV irradiation (365 nm) of caged prodrugs can completely restore the inhibitory potency of vemurafenib in proliferative and signal transduction assays. The cellular growth assays indicated that the applied UV dosage is well-tolerated by the melanoma cells.

There are already some examples of caged kinase inhibitors described in the literature.[7,31] However, the herein presented caged compounds are, to the best of our knowledge, the first

DOI: 10.1021/acschembio.5b00174
ACS Chem. Biol. 2015, 10, 2099−2107

photoactivatable derivatives of an approved small-molecule kinase inhibitor. Caged kinase inhibitors offer an exciting option for novel therapeutic applications. By targeted irradiation, it might be possible to release high concentrations of an active compound in a precisely controlled way in only appropriate sites afflicted by disease. With this approach of locally restricted activation, it is conceivable that systemic side effects can be prevented and the incidence of acquired resistances, reduced. For instance, the paradoxic stimulation of ERK phosphorylation by vemurafenib in wild-type BRAF cells[12] could presumably be reduced by a caged inhibitor.

Actually, our study is complementary to application of UV light for medical/therapeutic purposes. For instance, the psoralen plus UV-A (PUVA) therapy has been applied in dermatology since the 1970s.[32] The fact that UV light can be carcinogenic is commonly known because of its DNA damaging effects, but this is only in the case of UVC and UVB radiation. In contrast, UVA irradiation (wavelengths above 320 nm) does not affect the genetic material and is therefore not harmful at low limited dosage.[33] The implementation of light for release of therapeutically active substances may be restricted due to low tissue penetration. Several solutions for this problem are possible: The required light could be transmitted to the site of interest via optical fibers or endoscopic probes. Moreover, in selected cases, adjacent areas could be illuminated during the surgery.

Besides the *o*-nitrobenzylic derivatives implemented in this study, a variety of PPGs are described in the literature.[2,6,34] By varying the PPG, the required wavelength can be adapted. The deepest permeation into biological tissue can be achieved by wavelengths within the biological optical window. Wavelengths around 800 nm should best meet this challenge.[35] Hence, two-photon excitation could be used, supposing that the caged compound is sensitive to two-photon excitation.[5]

For future therapeutic applications, biological effects of the cleaved PPG and the cyclic benzisoxazolidine intermediate should be thoroughly explored. UV irradiation of the herein utilized *o*-nitrobenzylic PPGs generates supposedly toxic nitroso compounds. In the presented cellular proliferation assays, the released 4,5-dimethoxy-2-nitroso-benzaldehyde (the cleaved DMNB) showed intrinsic toxicity only at concentrations above 10 μM. This might not be critical because the caged compounds could be applied at much lower concentrations. The caged vemurafenib derivatives exhibit antiproliferative effects already at concentrations around 0.1 μM. Therefore, there might still be a wide therapeutic window for possible applications. Due to its short half-life, the biological effect of the cyclic intermediate could not be explored in the described assays. Further investigations in cellular assays and animal studies could reveal the effects of cleaved PPGs on biological tissue more thoroughly.

In conclusion, we created novel caged derivatives of the approved kinase inhibitor vemurafenib and proved that these prodrugs can be photoactivated *in vitro*. Our straightforward workflow implemented (1) determination of suitable pharmacophore moieties by modeling, (2) testing the UV stability of the active inhibitor, (3) synthesis of caged prodrugs, (4) characterizing their photoactivation, and (5) evaluating their photoactivation *in vitro*. This rational approach can be used for the generation of other photoactivatable (kinase) inhibitors as well based on different precursors and caged by various PPGs. Additionally, caged kinase inhibitors represent a powerful biochemical tool for studying the kinetics and regulation of phosphorylation processes in signal transduction cascades. These events can be precisely triggered by a short laser impulse. On the other hand, caged kinase inhibitors create new possibilities for therapeutic applications. Profound research regarding the stability, bioavailability, and toxicity of the caged kinase inhibitors is required to ensure their medical applicability. Further cellular and animal studies are planned to address these questions.

■ ASSOCIATED CONTENT

Supporting Information

Figure S1: 2D ligand interaction diagram of vemurafenib in $BRAF^{V600E}$. Figure S2: Calibration curves of vemurafenib for HPLC analysis. Figure S3: UV stability of vemurafenib. Figure S4: UV sources. Figure S5: Technical setup and emission characteristics of the utilized UV sources. Figure S6: Synthesis of caged prodrugs. Figure S7: Modeled structures of proposed atropisomers of sulfonamide DMNPE protected vemurafenib. Figure S8: Chromatographic separation of DMNPE protected vemurafenib derivatives. Figure S9: UV/vis absorption spectra of key compounds. Figure S10: Photorelease of vemurafenib by caged prodrug **3** and cyclic benzisoxazolidine intermediate formation, photoactivation of vemurafenib prodrugs and azaindole derivatives, and stability of vemurafenib prodrugs in cellular growth medium. Figure S11: Effect of the photoreleased PPG on the cell proliferation of SKMel13 cells. Figure S12: Effect of compound **3** on the phosphorylation of ERK in SKMel13 cells. Figure S13: Effect of vemurafenib (**1**) and caged compounds **2** and **4** on the phosphorylation of Akt in SKMel13 cells. Figure S14: Effect of compound **3** on the phosphorylation of Akt in SKMel13 cells. Figure S15: Binding affinity curves of vemurafenib (**1**) and prodrugs **2**, **3**, and **4** toward $BRAF^{V600E}$. Table S1: Kinase profiling of vemurafenib (**1**) and prodrugs **2** and **4**. Table S2: Cytotoxic activity of vemurafenib (**1**) and prodrug **2** without and with UV irradiation toward $BRAF^{V600E}$-positive melanoma cell lines. Methods, chemical synthesis, and compound characterization. The Supporting Information is available free of charge on the ACS Publications website at DOI: 10.1021/acschembio.5b00174.

■ AUTHOR INFORMATION

Corresponding Author

*E-mail: cpeifer@pharmazie.uni-kiel.de.

Author Contributions

§R.H. and B.P. contributed equally to this work.

Notes

The authors declare no competing financial interest.

■ ACKNOWLEDGMENTS

We thank T. Behrendt, A. Döbber, U. Girreser, and M. Schütt for excellent technical and analytical assistance at the Institute of Pharmacy in Kiel, Germany. We gratefully acknowledge the help of D. Schollmeyer, Institute for Organic Chemistry in Mainz, Germany, for X-ray analysis of compounds. Furthermore, we thank K. Dissanayaka from the MRC Protein Phosphorylation Unit at University of Dundee, Scotland, UK, for providing us with SKMel13 cells. We wish to thank the staff at the National Centre for Protein Kinase Profiling in Dundee for undertaking kinase specificity screening. Financial support by DFG (German Research Society) grant PE 1605/2-1 is greatly acknowledged.

DOI: 10.1021/acschembio.5b00174
ACS Chem. Biol. 2015, 10, 2099−2107

REFERENCES

(1) Levitzki, A. (2013) Tyrosine kinase inhibitors: views of selectivity, sensitivity, and clinical performance. *Annu. Rev. Pharmacol. Toxicol. 53*, 161−185.

(2) Klán, P., Solomek, T., Bochet, C. G., Blanc, A., Givens, R., Rubina, M., Popik, V., Kostikov, A., and Wirz, J. (2013) Photoremovable protecting groups in chemistry and biology: reaction mechanisms and efficacy. *Chem. Rev. 113*, 119−191.

(3) Kaplan, J. H., Forbush, B., and Hoffman, J. F. (1978) Rapid photolytic release of adenosine 5′-triphosphate from a protected analog: utilization by the sodium:potassium pump of human red blood cell ghosts. *Biochemistry 17*, 1929−1935.

(4) Velema, W. A., Szymanski, W., and Feringa, B. L. (2014) Photopharmacology: beyond proof of principle. *J. Am. Chem. Soc. 136*, 2178−2191.

(5) Ellis-Davies, G. C. R. (2007) Caged compounds: photorelease technology for control of cellular chemistry and physiology. *Nat. Methods 4*, 619−628.

(6) Mayer, G., and Heckel, A. (2006) Biologically active molecules with a "light switch". *Angew. Chem, Int. Ed. 45*, 4900−4921.

(7) Morckel, A. R., Lusic, H., Farzana, L., Yoder, J. A., Deiiters, A., and Nascone-Yoder, N. M. (2012) A photoactivatable small-molecule inhibitor for light-controlled spatiotemporal regulation of Rho kinase in live embryos. *Development 139*, 437−442.

(8) Li, H., Hah, J.-M., and Lawrence, D. S. (2008) Light-mediated liberation of enzymatic activity: "small molecule" caged protein equivalents. *J. Am. Chem. Soc. 130*, 10474−10475.

(9) Curley, K., and Lawrence, D. S. (1999) Caged regulators of signaling pathways. *Pharmacol. Ther. 82*, 347−354.

(10) Veldhuyzen, W. F., Nguyen, Q., McMaster, G., and Lawrence, D. S. (2003) A light-activated probe of intracellular protein kinase activity. *J. Am. Chem. Soc. 125*, 13358−13359.

(11) Wang, Q., Dai, Z., Cahill, S. M., Blumenstein, M., and Lawrence, D. S. (2006) Light-regulated sampling of protein tyrosine kinase activity. *J. Am. Chem. Soc. 128*, 14016−14017.

(12) Bollag, G., Tsai, J., Zhang, J., Zhang, C., Ibrahim, P., Nolop, K., and Hirth, P. (2012) Vemurafenib: the first drug approved for BRAF-mutant cancer. *Nat. Rev. Drug Discovery 11*, 873−886.

(13) Flaherty, K. T., Puzanov, I., Kim, K. B., Ribas, A., McArthur, G. A., Sosman, J. A., O'Dwyer, P. J., Lee, R. J., Grippo, J. F., Nolop, K., and Chapman, P. B. (2010) Inhibition of mutated, activated BRAF in metastatic melanoma. *N. Engl. J. Med. 363*, 809−819.

(14) Chapman, P. B., Hauschild, A., Robert, C., Haanen, J. B., Ascierto, P., Larkin, J., Dummer, R., Garbe, C., Testori, A., Majo, M., Hogg, D., Lorigan, P., Lebbe, C., Jouary, T., Schadendorf, D., Ribas, A., ÓDay, S. J., Sosman, J. A., Kirkwood, J. M., Eggermont, A. M. M., Dreno, B., Nolop, K., Li, J., Nelson, B., Hou, J., Lee, R. J., Flaherty, K. T., and McArthur, G. A. (2011) Improved survival with vemurafenib in melanoma with BRAF V600E mutation. *N. Engl. J. Med. 364*, 2507−2516.

(15) Sosman, J. A., Kim, K. B., Schuchter, L., Gonsalez, R., Pavlick, A. C., Weber, J. S., McArthur, G. A., Hutson, T. E., Moschos, S. J., Flaherty, K. T., Hersey, P., Kefford, R., Lawrence, D., Puzanov, I., Lewis, K. D., Amaravadi, R. K., Chmielowski, B., Lawrence, H. J., Shyr, Y., Ye, F., Li, J., Nolop, K. B., Lee, R. J., Joe, A. K., and Ribas, A. (2012) Survival in BRAF V600-mutant advanced melanoma treated with vemurafenib. *N. Engl J. Med. 366*, 707−714.

(16) Jang, S., and Atkins, M. B. (2014) Treatment of BRAF-mutant melanoma: the role of vemurafenib and other therapies. *Clin. Pharmacol. Ther. 95*, 24−31.

(17) Swaika, A., Crozier, J. A., and Joseph, R. W. (2014) Vemurafenib: an evidence-based review of its clinical utility in the treatment of metastatic melanoma. *Drug Des., Dev. Ther. 8*, 775−787.

(18) Shi, H., Moriceau, G., Kong, X., Lee, M.-K., Lee, H., Koya, R. C., Ng, C., Chodon, T., Scolyer, R. A., Dahlman, K. B., Sosman, J. A., Kefford, R. F., Long, G. V., Nelson, S. F., Ribas, A., and Lo, R. S. (2012) Melanoma whole-exome sequencing identifies (V600E)B-RAF amplification-mediated acquired B-RAF inhibitor resistance. *Nat. Commun. 3*, 724−740.

(19) Poulikakos, P. I., Persaud, Y., Janakiraman, M., Kong, X., Ng, C., Moriceau, G., Shi, H., Atefi, M., Titz, B., Gabay, M. T., Salton, M., Dahlman, K. B., Tadi, M., Wargo, J. A., Flaherty, K. T., Kelley, M. C., Misteli, T., Chapman, P. B., Sosman, J. A., Graeber, T. G., Ribas, A., Lo, R. S., Rosen, N., and Solit, D. B. (2011) RAF inhibitor resistance is mediated by dimerization of aberrantly spliced BRAF(V600E). *Nature 480*, 387−390.

(20) Johannessen, C. M., Boehm, J. S., Kim, S. Y., Thomas, S. R., Wardwell, L., Johnson, L. A., Emery, C. M., Stransky, N., Cogdill, A. P., Barretina, J., Caponigro, G., Hieronymus, H., Murray, R. R., Salehi-Ashtiani, K., Hill, D. E., Vidal, M., Zhao, J. J., Yang, X., Alkan, O., Kim, S., Harris, J. L., Wilson, C. J., Myer, V. E., Finan, P. M., Root, D. E., Roberts, T. M., Golub, T., Flaherty, K. T., Dummer, R., Weber, B. L., Sellers, W. R., Schlegel, R., Wargo, J. A., Hahn, W. C., and Garraway, L. A. (2010) COT drives resistance to RAF inhibition through MAP kinase pathway reactivation. *Nature 468*, 968−972.

(21) Shi, H., Kong, X., Ribas, A., and Lo, R. S. (2011) Combinatorial treatments that overcome PDGFRβ-driven resistance of melanoma cells to V600EB-RAF inhibition. *Cancer Res. 71*, 5067−5074.

(22) Villanueva, J., Vultur, A., Lee, J. T., Somasundaram, R., Fukunaga-Kalabis, M., Cipolla, A. K., Wubbenhorst, B., Xu, X., Gimotty, P. A., Kee, D., Santiago-Walker, A. E., Letrero, R., DÁndrea, K., Pushparajan, A., Hyden, J. E., Brown, K. D., Laquerre, S., McArthur, G. A., Sosman, J. A., Nathanson, K. L., and Herlyn, M. (2010) Acquired resistance to BRAF inhibitors mediated by a RAF kinase switch in melanoma can be overcome by cotargeting MEK and IGF-1R/PI3K. *Cancer Cell 18*, 683−695.

(23) Bollag, G., Hirth, P., Tsai, J., Zhang, J., Ibrahim, P. N., Cho, H., Spevak, W., Zhang, C., Zhang, Y., Habets, G., Burton, E. A., Wong, B., Tsang, G., West, B. L., Powell, B., Shellooe, R., Marimuthu, A., Nguyen, H., Zhang, K. Y. J., Artis, D. R., Schlessinger, J., Su, F., Higgins, B., Iyer, R., DÁndrea, K., Koehler, A., Stumm, M., Lin, P. S., Lee, R. J., Grippo, J., Puzanov, I., Kim, K. B., Ribas, A., McArthur, G. A., Sosman, J. A., Chapman, P. B., Flaherty, K. T., Xu, X., Nathanson, K. L., and Nolop, K. (2010) Clinical efficacy of a RAF inhibitor needs broad target blockade in BRAF-mutant melanoma. *Nature 467*, 596−599.

(24) Dar, A. C., and Shokat, K. M. (2011) The evolution of protein kinase inhibitors from antagonists to agonists of cellular signaling. *Annu. Rev. Biochem. 80*, 769−795.

(25) Rabiller, M., Getlik, M., Klüter, S., Richters, A., Tückmantel, S., Simard, J. R., and Rauh, D. (2010) Proteus in the world of proteins: conformational changes in protein kinases. *Arch. Pharm. (Weinheim, Ger.) 343*, 193−206.

(26) Collins, I., and Workman, P. (2006) Design and development of signal transduction inhibitors for cancer treatment: experience and challenges with kinase targets. *Curr. Signal Transduction Ther. 1*, 13−23.

(27) Dissanayake, K., Toth, R., Blakey, J., Olsson, O., Campbell, D. G., Prescott, A. R., and MacKintosch, C. (2011) ERK/p90(RSK)/14-3-3 signalling has an impact on expression of PEA3 Ets transcription factors via the transcriptional repressor capicúa. *Biochem. J. 433*, 515−525.

(28) Yang, H., Higgins, B., Kolinsky, K., Packman, K., Go, Z., Iyer, R., Kolis, S., Zhao, S., Lee, R., Grippo, J. F., Schostack, K., Simcox, M. E., Heimbrook, D., Bollag, D., and Su, F. (2010) RG7204 (PLX4032), a selective BRAFV600E inhibitor, displays potent antitumor activity in preclinical melanoma models. *Cancer Res. 70*, 5518−5527.

(29) Lee, J. T., Li, L., Brafford, P. A., van den Eijnden, M., Halloran, M. B., Sproesser, K., Haass, N. K., Smalley, K. S. M., Tsai, J., Bollag, G., and Herlyn, M. (2010) PLX4032, a potent inhibitor of the B-Raf V600E oncogene, selectively inhibits V600E-positive melanomas. *Pigm. Cell Melanoma Res. 23*, 820−827.

(30) Søndergaard, J. N., Nazarian, R., Wang, Q., Guo, D., Hsueh, T., Mok, S., Sazegar, H., MacConail, L. E., Barretina, J. G., Kehoe, S. M., Attar, N., von Euw, E., Zuckerman, J. E., Chmielowski, B., Comin-Anduix, B., Koya, R. C., Mischel, P. S., Lo, R. S., and Ribas, A. (2010) Differential sensitivity of melanoma cell lines with BRAFV600E mutation to the specific Raf inhibitor PLX4032. *J. Trans. Med. 8*, 39.

DOI: 10.1021/acschembio.5b00174
ACS Chem. Biol. 2015, 10, 2099−2107

(31) Wood, J. S., Koszelak, M., Liu, J., and Lawrence, D. S. (1998) A caged protein kinase inhibitor. *J. Am. Chem. Soc. 120*, 7145−7146.
(32) Morison, W. L., Parrish, J. A., and Fitzpatrick, T. B. (1978) Controlled study of PUVA and adjunctive topical therapy in the management of psoriasis. *Br. J. Dermatol. 98*, 125−132.
(33) Matsumura, Y., and Ananthaswamy, H. N. (2004) Toxic effects of ultraviolet radiation on the skin. *Toxicol. Appl. Pharmacol. 195*, 298−308.
(34) Pelliccioli, A. P., and Wirz, J. (2002) Photoremovable protecting groups: reaction mechanisms and applications. *Photochem. Photobiol. Sci. 1*, 441−458.
(35) Byrnes, K. R., Waynant, R. W., Ilev, I. K., Wu, X., Barna, L., Smith, K., Heckert, R., Gerst, H., and Anders, J. J. (2005) Light promotes regeneration and functional recovery and alters the immune response after spinal cord injury. *Lasers Surg. Med. 36*, 171−185.

DOI: 10.1021/acschembio.5b00174
ACS Chem. Biol. 2015, 10, 2099−2107